물리탐사
Vol. 2, No. 2, 1999, p. 86~95

Three-dimensional Cross-hole EM Modeling using the Extended Born Approximation

Lee, Seong Kon[1], Kim, Hee Joon[2] and Suh, Jung Hee[3]

확장 Born 근사에 의한 시추공간 3차원 전자탐사 모델링

이성곤 · 김희준 · 서정희

Abstract : This paper presents an efficient three-dimensional (3-D) modeling algorithm using the extended approximation to an electric field integral equation. Numerical evaluations of Green's tensor integral are performed in the spatial wavenumber domain. This approach makes it possible to reduce computing time, to handle smoothly varying conductivity model and to remove singularity problems encountered in the integration of Green's tensor at a source point. The responses obtained by 3-D modeling algorithm developed in this study are compared with those by the full integral equation for a thin-sheet EM scattering. The extensive analyses on the performance of modeling algorithm are made with the conductivity contrasts and source frequencies. These results show that the modeling algorithm are accurate up to the conductivity contrast of 1:16 and the frequency range of 100 Hz-100 kHz. The extended Born approximation, however, may produce inaccurate results for some source and model configurations in which the electric field is discontinuous across the conductivity boundary. We performed the modeling of a composite model of which conductivity varies continuously and this shows the modeling algorithm developed in this study is efficient for 3-D EM modeling. For a cross-hole source-receiver configuration a composite model of which conductivity varies continuously can be successfully simulated using this algorithm.

요 약 : 이 연구에서는 적분방정식의 근사해를 이용한 3차원 모델링 알고리듬을 구성하고 그 효율성을 분석하였다. 전기장 적분방정식에 확장 Born 근사(extended Born approximation)를 적용시켜 알고리듬을 구성하였으며 모델링의 계산 속도를 향상시키기 위하여 Green 텐서 적분을 공간 주파수 영역에서 수행하였다. 이 방법은 연속 함수로 표현되는 전기전도도를 갖는 이상체에 대한 모델 계산을 가능하게 하고, Green 텐서 적분시 발생하는 특이치 문제가 발생하지 않는 장점이 있다. 얇은 전도체에 대한 모델링 계산 결과를 적분방정식의 해와 비교하여 알고리듬의 타당성을 검증하였다. 전기전도도 물성차, 사용 송신원의 주파수에 따른 개발된 알고리듬의 분석을 통하여 물성차 1:16 정도, 사용주파수는 100 Hz-100 kHz 까지 정확한 결과를 얻었다. 그러나, 확장 Born 근사는 송신원과 모델의 상대적인 위치에 따라 오차를 나타내었다. 한편, 연속적인 전기전도도 함수를 갖는 모델에 대한 이 알고리듬의 적용성를 알아보기 위하여 서로 다른 전기전도도를 갖는 두 이상체가 접합한 모델에 대하여 적분방정식의 해와 비교하였으며 양호한 결과를 나타내었다.

Keywords : 3-D modeling, integral equation, Green's tensor, spatial wavenumber, extended Born approximation

Introduction

Electromagnetic (EM) exploration methods are useful for detecting subsurface targets having anomalous electrical properties such as ore deposits, geothermal reservoirs, ground water, and environmental contamination plumes. The fundamental principle underlying the conventional EM methods is the diffusive nature of EM fields in the subsurface media. Like many other physical properties measured with the geophysical methods, the electrical conductivity distribution in the earth is very complicated and mostly random. The major difficulty in these exploration tasks is the lack of effective interpretation tools (Lee, 1991).

Numerical solutions have been successfully obtained using finite difference method (Hermance, 1982; Oristaglio and Hohmann, 1984), finite element method (Coggon, 1971; Pridmore *et al.*, 1981), integral equation method (Wannamaker *et al.*, 1984; Walker and West, 1991; Xiong, 1992) or

*1999년 4월 6일 접수
1) Seoul National University (서울대학교 공학연구소)
2) Pukyong National University (부경대학교 탐사공학과)
3) Civil, Urban & Geosystem Eng., Seoul National University (서울대학교 지구환경시스템공학부)

some combinations of these methods (Lee *et al.*, 1981). However, any rigorous numerical modeling of EM scattering problems, especially in the case of 3-D structures, is very time consuming and takes a large amount of computer memory. As a result, 3-D EM data analysis is very difficult unless the algorithm is implemented on a massively parallel computing machine or a multiple processor environment (Alumbaugh and Newman, 1995; Xie *et al.*, 1995). The use of these algorithms, however, is very restricted for the analysis of 3-D EM field data.

Alternative approaches to the 3-D EM modeling are to seek an approximate, but reasonably accurate within measurement errors. These solutions are mostly based on the Born approximations. Many algorithms have been developed for both modeling and inversion using the Born approximation (Zhou *et al.*, 1993; Alumbaugh and Morrison, 1993). The Born approximation technique, however, may be inaccurate for high conductivity contrast and at higher frequencies. Habashy *et al.* (1993) suggested a new method called the extended Born approximation method in which the electric field is linearized locally in inhomogeneities. The 2-D and 2.5-D numerical algorithms have been developed based on this approximation (Torres-Verdin and Habashy, 1994, 1995; Miller and Willsky, 1996; Cho and Suh, 1998) and successfully approximated the true solution for some cases. Tseng *et al.* (1996) improved computational efficiency of the extended Born approximation algorithms by evaluating the integrals in spatial wavenumber domain.

In this study, an efficient 3-D modeling algorithm has been developed using the extended Born approximation suggested by Habashy *et al.* (1993) and its efficiency is analyzed. To speed up this modeling algorithm the spatial wavenumber approach suggested by Tseng *et al.* (1996) is implemented. Numerical evaluation of Green's tensor integral in the wavenumber domain is useful to reduce the computation time and to simulate the response of a smoothly varying conductivity model. The extended Born approximation, however, may produce inaccurate results for some source and model configurations. All results obtained by the developed algorithm are compared with the results obtained by the thin sheet modeling scheme (Song and Lee, 1998).

Basic Theory

Integral equation

We here briefly review some basic aspects of integral equation. Many authors have dealt with this subject (Hohmann, 1975; Kong, 1986; Habashy *et al.*, 1993). Suppose that a scatterer or an object be embedded in a background medium. At any location $\mathbf{r}$ in a medium V, $\mathbf{r} \in V$, the electric field satisfies vector Helmholtz equation. In the frequency domain under the $\exp(i\omega t)$ time dependence, the vector Helmholtz equation can be represented as

$$\nabla\times\nabla\times\mathbf{E}(\mathbf{r})-k^2\mathbf{E}(\mathbf{r})=-i\omega\mu\mathbf{J}_e(\mathbf{r}), , \tag{1}$$

where $\mathbf{E}(\mathbf{r})$ is the electric field intensity (V/m) and $\mathbf{J}_e(\mathbf{r})$ is the impressed electric current density (A/m^2). The impressed electric current density $\mathbf{J}_e(\mathbf{r})$ could be written as $Id\mathbf{l}\delta(\mathbf{r}-\mathbf{r}_s)$ in which the symbol $Id\mathbf{l}$ denotes infinitesimal current dipole source located at $\mathbf{r}_s$. In addition, k is the complex propagation constant at $\mathbf{r}$ given by

$$k^2(\mathbf{r})=-i\omega\mu\{\sigma(\mathbf{r})+i\omega\varepsilon(\mathbf{r})\}=-\hat{z}\hat{y}(\mathbf{r}), \tag{2}$$

where $\hat{z}$ $(=i\omega\mu)$ is the impedivity and $\hat{y}$ $(=\sigma+i\omega\varepsilon)$ is the admittivity (Ward and Hohmann, 1987). In this equation, $\sigma(\mathbf{r})$ is the electric conductivity (S/m), $\varepsilon(\mathbf{r})$ is the dielectric permittivity (F/m) at $\mathbf{r}$ in the medium, ω is the angular frequency and μ is the magnetic permeability (H/m) which is generally assumed to be the value of free space, $\mu_0(=4\pi\times 10^{-7})$, respectively.

The solution of equation (1) can be obtained in terms of the tensor Green's function that satisfies an equation

$$\nabla\times\nabla\times\underline{\underline{\mathbf{G}}}_E(\mathbf{r},\mathbf{r}')-k_b^2\underline{\underline{\mathbf{G}}}_E(\mathbf{r},\mathbf{r}') = \underline{\underline{\mathbf{I}}}\delta(\mathbf{r}-\mathbf{r}'), \tag{3}$$

where $\underline{\underline{\mathbf{G}}}_E$ is the electric Green's tensor which relates the electric field at $\mathbf{r}$ to a unit current source located at $\mathbf{r}'$ and $\underline{\underline{\mathbf{I}}}$ is an identity tensor. The k_b is the complex propagation constant in the background medium given by

$$k_b^2(\mathbf{r})=-i\omega\mu_0(\sigma_b+i\omega\varepsilon_b)=-\hat{z}\hat{y}_b, \tag{4}$$

where σ_b is the electric conductivity (S/m) and ε_b is the permittivity of the background medium. For a homogeneous whole space background, the tensor Green's function $\underline{\underline{\mathbf{G}}}_E$ is

$$\underline{\underline{\mathbf{G}}}_E(\mathbf{r},\mathbf{r}')=\left[\underline{\underline{\mathbf{I}}}+\frac{1}{k_b^2}\nabla\nabla\right]g(\mathbf{r},\mathbf{r}'), \tag{5}$$

where $g(\mathbf{r},\mathbf{r}')$ is the scalar Green's function represented by

$$g(\mathbf{r},\mathbf{r}')=\frac{e^{-ik_b|\mathbf{r}-\mathbf{r}'|}}{4\pi|\mathbf{r}-\mathbf{r}'|}. \tag{6}$$

The solution of equation (1) is given by

$$\mathbf{E}(\mathbf{r})=\mathbf{E}_b(\mathbf{r})-\hat{z}\int_V \underline{\underline{\mathbf{G}}}_E(\mathbf{r},\mathbf{r}')\cdot\Delta\hat{y}(\mathbf{r}')\mathbf{E}(\mathbf{r}')d\mathbf{r}'. \tag{7}$$

where

$$\Delta\hat{y}(\mathbf{r})=(\sigma(\mathbf{r})+i\omega\varepsilon(\mathbf{r}))-(\sigma_b+i\omega\varepsilon_b)=\hat{y}(\mathbf{r})-\hat{y}_b. \tag{8}$$

Equation (7) is the fundamental integral equation of EM scattering problem which is the Fredholm equation of the second kind and non-linear in $\Delta\hat{y}(\mathbf{r})$. The total electric field $\mathbf{E}(\mathbf{r})$ in the inhomogeneity can be represented as the sum of the primary (incident) field $\mathbf{E}_b(\mathbf{r})$ and the secondary (scattered) field $\mathbf{E}_s(\mathbf{r})$ which is generated by the scattering cur-

rent induced inside the conducting object (Jackson, 1971). The magnetic field in the receiver is then given by

$$\mathbf{H}(\mathbf{r})=\mathbf{H}_b(\mathbf{r})-\hat{z}\int_V \underline{\underline{\mathbf{G}}}_H(\mathbf{r},\mathbf{r}')\cdot\Delta\hat{y}(\mathbf{r}')\mathbf{E}(\mathbf{r}')d\mathbf{r}', \quad (9)$$

where $\underline{\underline{\mathbf{G}}}_H$ is the magnetic tensor Green's function defined by

$$\underline{\underline{\mathbf{G}}}_H(\mathbf{r},\mathbf{r}')=-\frac{\nabla\times\underline{\underline{\mathbf{G}}}_E(\mathbf{r},\mathbf{r}')}{\hat{z}}. \quad (10)$$

Extended Born approximation

Born approximation method replaces the total field in the integrand of equation (7) with the primary (incident) field and thus makes it easier to solve. Habashy *et al.* (1993) suggested an alternate way to linearize the equation (7) as

$$\mathbf{E}(\mathbf{r})=\underline{\underline{\Gamma}}(\mathbf{r})\cdot\left[\mathbf{E}_b(\mathbf{r})-\hat{z}\int_V \underline{\underline{\mathbf{G}}}_E(\mathbf{r},\mathbf{r}')\cdot\Delta\hat{y}(\mathbf{r}')\{\mathbf{E}(\mathbf{r}')-\mathbf{E}(\mathbf{r})\}d\mathbf{r}'\right], \quad (11)$$

where $\underline{\underline{\Gamma}}(\mathbf{r})$ is called a scattering tensor or depolarization tensor defined as

$$\underline{\underline{\Gamma}}(\mathbf{r})=\left[\underline{\underline{\mathbf{I}}}+\hat{z}\int_V \underline{\underline{\mathbf{G}}}_E(\mathbf{r},\mathbf{r}')\Delta\hat{y}(\mathbf{r}')d\mathbf{r}'\right]^{-1} \quad (12)$$

and $\underline{\underline{\mathbf{I}}}$ is a 3×3 identity tensor. An approximation to the total electric field $\mathbf{E}(\mathbf{r})$ is in turn made by ignoring the second term enclosed by the brace in the right-hand side of the equation (11)

$$\mathbf{E}(\mathbf{r})\approx\underline{\underline{\Gamma}}(\mathbf{r})\cdot\mathbf{E}_b(\mathbf{r}). \quad (13)$$

This method is called the extended Born approximation or localized non-linear approximation and known to be accurate if the following condition is satisfied

$$|\mathbf{E}_b(\mathbf{r})|\gg\left|\hat{z}\int_V \underline{\underline{\mathbf{G}}}_E(\mathbf{r},\mathbf{r}')\Delta\hat{y}(\mathbf{r}')\{\mathbf{E}(\mathbf{r}')-\mathbf{E}(\mathbf{r})\}d\mathbf{r}'\right|. \quad (14)$$

It is apparent that the dominant contribution to the integral in equation (7) comes from the points in the vicinity of $\mathbf{r}'=\mathbf{r}$ because of the singular nature of a Green's tensor $\underline{\underline{\mathbf{G}}}_E(\mathbf{r},\mathbf{r}')$ at $\mathbf{r}'=\mathbf{r}$. The integral in equation (14), however, is expected to be very small because $\mathbf{E}(\mathbf{r}')$-$\mathbf{E}(\mathbf{r})$ is zero where $\underline{\underline{\mathbf{G}}}_E(\mathbf{r},\mathbf{r}')$ is singular at $\mathbf{r}'=\mathbf{r}$ (Habashy *et al.*, 1993).

Numerical implementation of 3-D modeling algorithm using the extended Born approximation

The use of integral equation method in 3-D numerical modeling is generally limited to specific models such as sphere, cylinder or cubic. For 3-D electromagnetic modeling by using even approximate solutions to integral equation, the computing time for evaluating a scattering tensor increases dramatically as the number of cells increases. Furthermore, its efficiency must be significantly improved in the view of computing time and the capability of describing a model in order to use the 3-D modeling algorithm for the inversion of 3-D EM data. The emphasis was put on the two points in developing of the computation algorithm. The first is to enhance the capability of describing shape of model and the second is to reduce computation time.

Model construction

The modeling algorithms developed in this study are based on the integral equation method. Unlike conventional integral equation method, it is assumed that conductivity distribution of an anomalous body may be constructed by a smooth function of space coordinate, not by a specific model. Fig. 1 shows the conceptual model adopted in this study. It is assumed that 3-D conductivity distribution can be constructed by a number of functions on the 2-D planes that are normal to the vertical direction. As shown in Fig. 1, the modeling region is defined by the 2-D planes vertical to z-axis. On each plane, 2-D conductivity distribution function is to be sampled in x and y direction. This model description is reasonable and physically meaningful in that the conductivity of the earth will not change abruptly but vary smoothly and that most of inversion algorithms now tend to incorporate smoothness constraints or regularization (Constable *et al.*, 1987). It is possible to say that this assumption will be especially useful in utilizing this algorithm for the inversion of 3-D EM data.

Green's tensor integral

As mentioned earlier, computing time for evaluating a scattering tensor increases dramatically as the number of

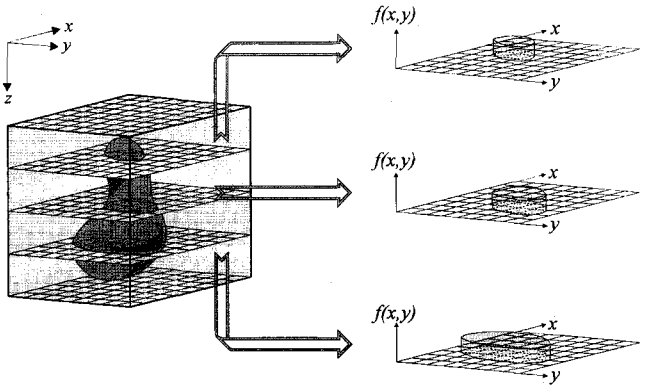

Fig. 1. Conceptual sketch of model construction for numerical calculation. It is assumed that the three-dimensional volume conductivity distribution (left) may be constructed by 2-D functions (right) at the sampling planes normal to z-axis.

blocks increases. One needs to seek a way of reducing the computing time in 3-D modeling. This can be achieved by performing the integration of a Green's tensor integral in the spatial wavenumber domain and then we can enjoy the efficiency of fast Fourier transform (FFT). This approach, furthermore, is favorable to the assumption of model construction adopted in this study. Such a technique was introduced by Lee (1991) and recently reviewed by Tseng *et al.* (1996).

Considering the integral in equation (7) or (9), one can write each component of integral in general form as

$$\Omega_i(\mathbf{r})=\int_V G_{ij}(\mathbf{r},\mathbf{r}')\Lambda_j(\mathbf{r}')d\mathbf{r}' \quad (i,j=x,y,z), \tag{15}$$

or more explicitly,

$$\Omega_i(x, y, z)=\iiint_V G_{ij}(x-x', y-y', z-z')\Lambda_j(x',y',z')dx'dy'dz' , \tag{16}$$

One can see that equation (15) or (16) is a convolution of a Green's function and a function Λ_j in the space domain. Evaluation of this integral can be very efficiently carried out in the wavenumber domain by using convolution theorem of Fourier transform. Rewriting equation (16) in terms of Fourier transform pairs, one has

$$\Omega_i(x,y,z)=\frac{1}{4\pi^2}$$

$$\int_Z\left[\int_{-\infty}^{\infty}\int_{-\infty}^{\infty}\tilde{G}_{ij}(k_x,k_y,z-z')\tilde{\Lambda}_j(k_x,k_y,z')e^{i(k_xx+k_yy)}dk_xdk_y\right]dz', \tag{17}$$

where k_x and k_y are the horizontal wavenumbers in x and y direction, respectively. As a result, once the double integral in x and y coordinates is evaluated in the wavenumber domain via FFT, the triple volume integral is reduced to the ordinary integration in z only. The convolution relationship still holds in horizontal coordinates (x, y) when the earth is layered.

This approach has distinctive advantages. Computing time is reduced dramatically because the convolution is simplified to a multiplication and tensor Green's functions are in simple algebraic form in wavenumber domain (Appendix) and thus make the calculation easier than in space domain. The singularity problem encountered in the calculation of the depolarization tensors due to a singular nature of the Green's function can be easily handled in wavenumber domain. The singularity at $\mathbf{r}=\mathbf{r}'$ will not occur for a whole space Green's tensor and could be easily handled for a half-space Green's function.

Results and Discussions

Validity of the modeling algorithm

The model used for the numerical verification is shown

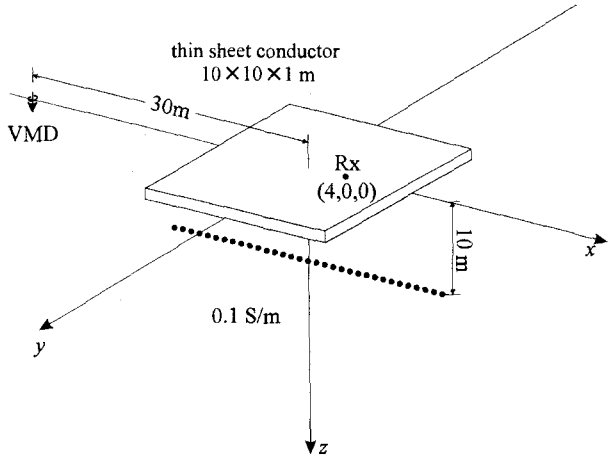

Fig. 2. Model used for the verification of performance of the modeling algoithms with the material property contrast. A receiver is located at (4,0,0) for comparison of internal vertical magnetic fields H_z^s. The receivers are located along the x-axis at depth z=10 m for comparison of external fields.

Fig. 2. A 10×10×1 m horizontal tabular conductor of 1 S/m is located in the whole space of 0.1 S/m. The conductivity contrast between the tabular conductor and the whole space is a factor of 10. The vertical magnetic dipole source operating at 5.6 kHz is located on the x-axis 30 m away from the center of the conductor. This model is the similar to the one studied in Tseng *et al.* (1996). The responses of this algorithm are compared with the results obtained from WSHEET code (Song and Lee, 1998). This code improved the thin sheet algorithm of Weidelt's (1981) to incorporate double sheet model and extends the frequency range up to 100 MHz.

It is straightforward to predict the response of this configuration with the assumption of thin sheet approximation. Only the vertical magnetic field due to a vertical magnetic dipole will pass through the thin sheet conductor. As a result, the secondary electric field due to scattering current would have horizontal components and the only vertical component of a secondary magnetic field would be observed in x-y plane. Fig. 3 shows the real and imaginary components of the secondary vertical magnetic fields along the x-axis, which are obtained by applying the extended Born approximation to the internal electric field. The modeling algorithm using the extended Born approximation method in this study gives accurate approximations for the internal magnetic fields. These values are in good agreement with the results of those of WSHEET.

Dependence on the conductivity contrast

Born approximation assumes weak scattering and gives accurate estimates of the scattered field only when the contrasts in physical property and the size of a scatterer are

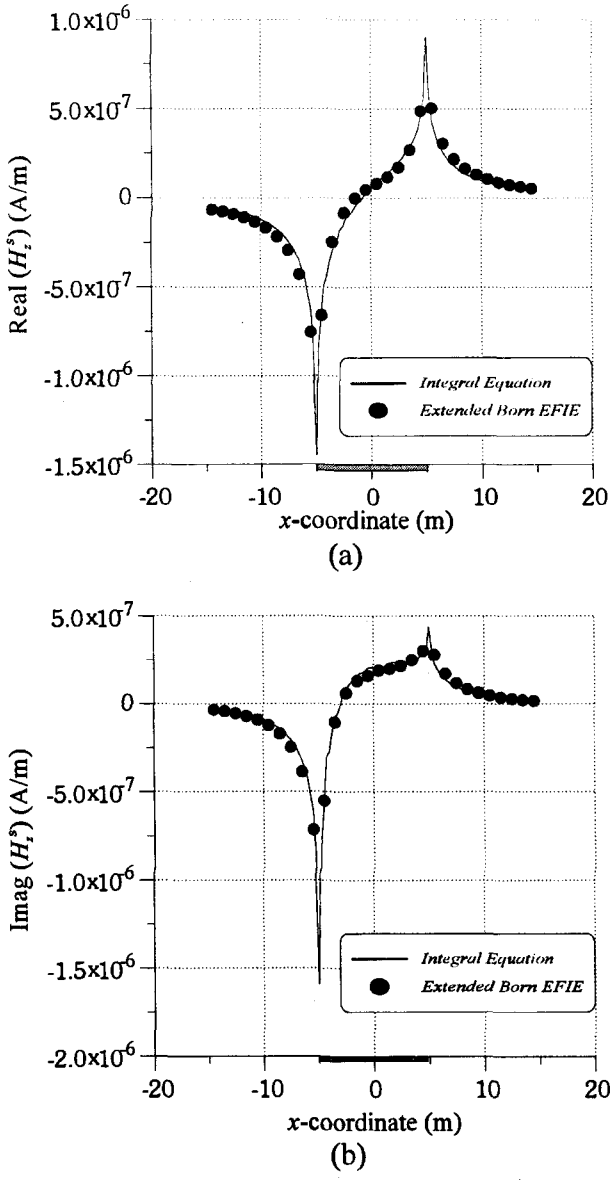

Fig. 3. Comparison of the secondary vertical magnetic fields H_z^s along the x-axis obtained from the extended Born approximation of EFIE and WSHEET. (a) Real component, (b) Imaginary component.

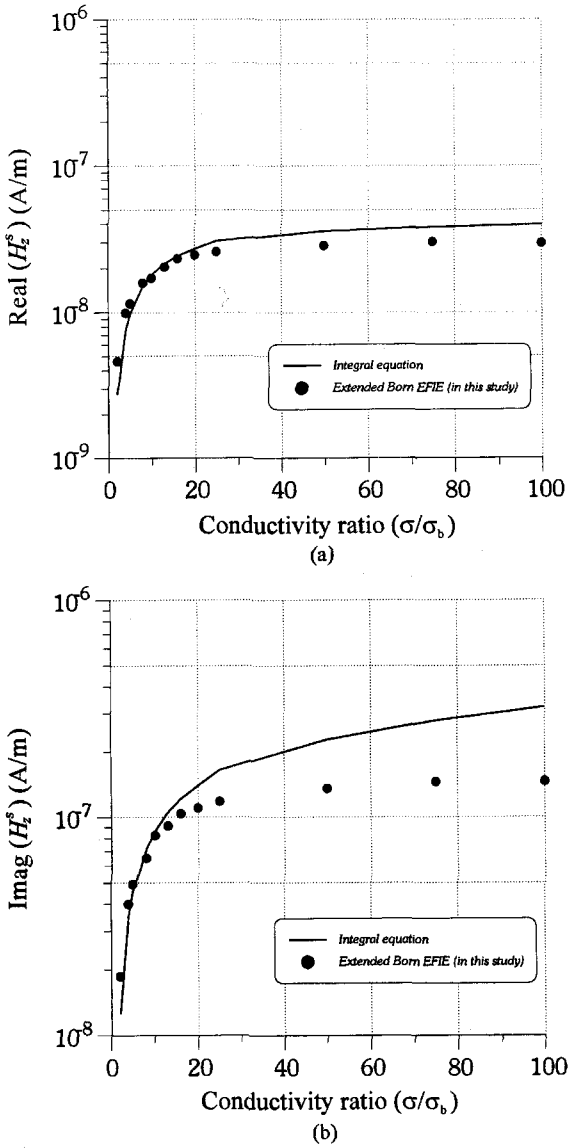

Fig. 4. Comparison of the secondary vertical magnetic field H_z^s obtained from the extended Born approximation of EFIE and WSHEFT as the material property contrast varies. The receiver is located at (4,0,0) inside the conductor.
(a) Real component, (b) Imaginary component

small. The conventional Born approximation is known to be accurate to within 20% error for 1 m sphere located 10 m from both the source and receiver for conductivity contrasts of 1:1.5 and the error grows rapidly to 400% at a conductivity contrast of 1:10 (Habashy *et al.* 1993). It is worthwhile to examine the accuracy of the algorithms developed in this study for a thin sheet conductor as the material contrast varies.

The model used for this test is the same as in Fig. 2 except the operating frequency of the VMD source is 1 kHz. The receiver is fixed in the conductor at $(x, y, z) = (4, 0, 0)$ to investigate the behavior of the modeling algorithm as conductivity contrast varies. The conductivity of background is kept constant value of 0.1 S/m. Fig. 4 shows the comparison of real and imaginary components of a secondary vertical magnetic field obtained from the extended Born approximation solution and WSHEET code as the contrast varies. The modeling algorithm developed in this study is accurate up to the contrast 1:16 within 5% error and becomes higher than that of WSHEET. Fig. 5 shows the real and imaginary components of secondary vertical magnetic fields along x-axis at depth 10 m (dotted line in Fig. 2) when the conductivity contrast is 13. The symbol denotes the extended Born approximation and the line denotes the results of WSHEET.

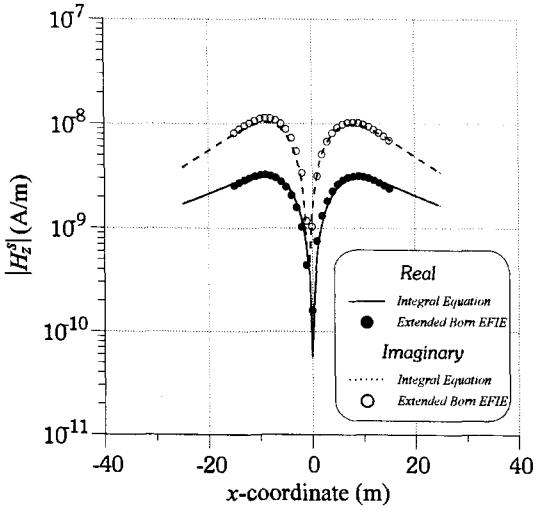

Fig. 5. Comparison of real and imaginary components of the external vertical magnetic fields H_z^s obtained from the extended Born approximation of EFIE and WSHEET. The receivers are located along the x-axis at depth 10 m as shown in Fig. 2.

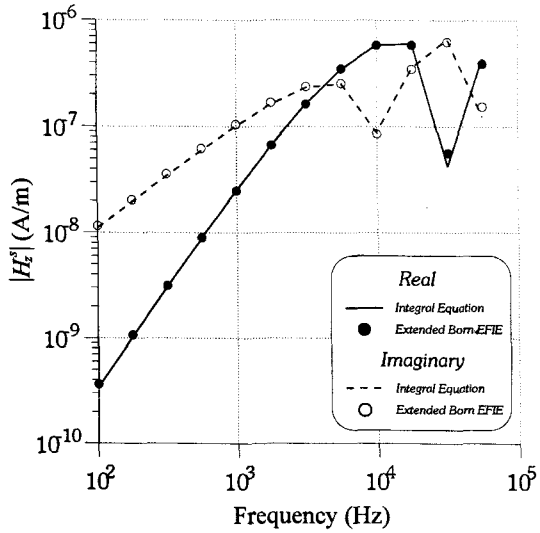

Fig. 6. Comparison of real and imaginary components of the secondary vertical magnetic fields H_z^s obtained from the extended Born approximation of EFIE and WSHEET as frequency varies. The receiver is located at (4,0,0) inside the conductor.

Dependence on source frequency

It is known that the accuracy of the Born approximation also depends on the frequency. Fig. 6 shows the comparison of real and imaginary components of a secondary vertical magnetic field as the frequency increases. The model is same as that in the comparison of conductivity contrast. The conductivity contrast is 10. Extended Born approximation shows accurate result over 3 decades of frequencies for this model. This approximation is accurate over the range from 100 Hz to 100 kHz.

A vertical fracture model

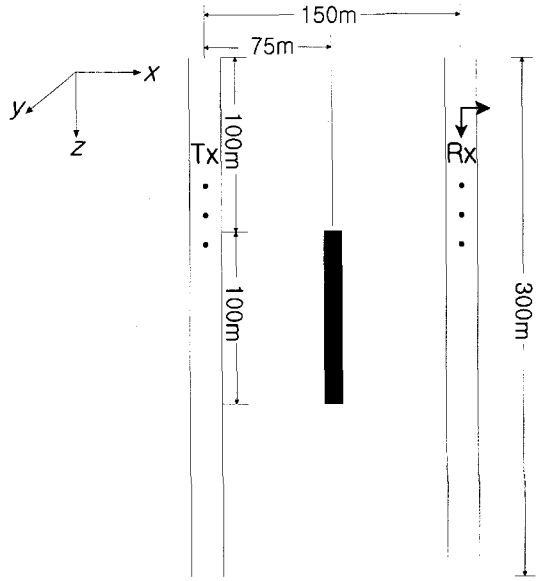

Fig. 7. A vertical fracture model between two boreholes in whole space. The conductivity of a vertical conductor is 1 S/m and 150 m, 100 m long in strike, dip direction, respectively. The sources and receivers are moving in parallel down the two boreholes.

Fig. 7 shows the vertical fracture model between two boreholes. Two boreholes are separated by 150 m in the whole space of 0.1 S/m. A vertical conductor is perpendicular to and symmetric about the plane defined by the boreholes. The conductivity of a vertical conductor is 1 S/m and 150 m, 100 m long in strike, dip direction, respectively. The source is either vertical magnetic dipole (VMD) or horizontal magnetic dipole (HMD) directed along the positive x-axis, which is operating at 1 kHz. The sources and receivers

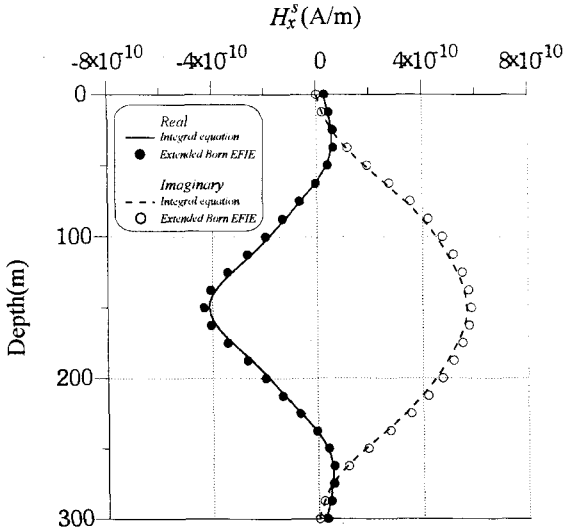

Fig. 8. Real and imaginary components of the horizontal magnetic fields H_z^s obtained from the extended Born approximation of EFIE and WSHEET due to a horizontal magnetic dipole source.

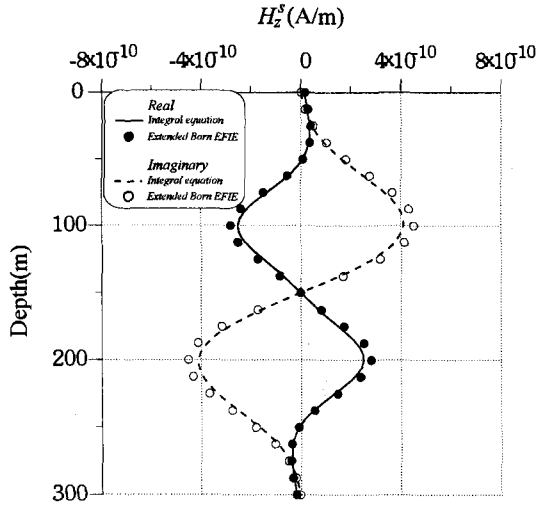

Fig. 9. Real and imaginary components of the vertical magnetic field H_z^s obtained from the extended Born approximation of EFIE and WSHEET due to a horizontal magnetic dipole source.

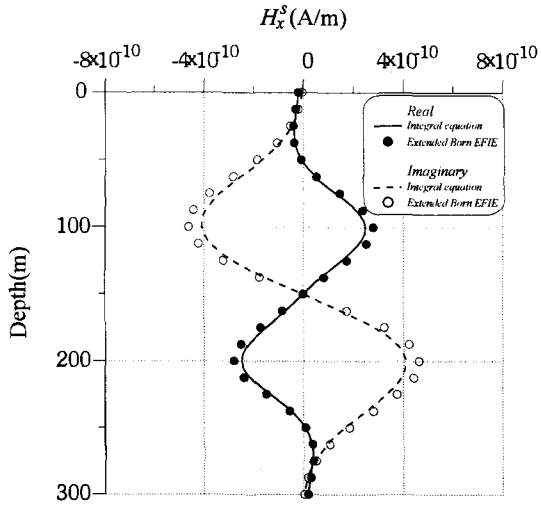

Fig. 10. Real and imaginary components of the horizontal magnetic fields H_z^s obtained from the extended Born approximation of EFIE and WSHEET due to a vertical magnetic dipole source.

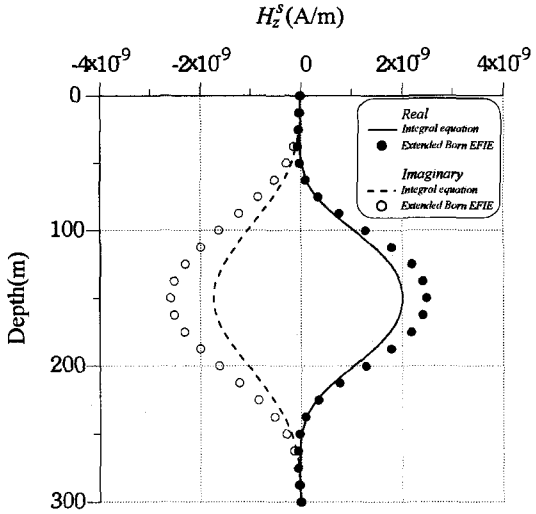

Fig. 11. Real and imaginary components of the vertical magnetic fields H_z^s obtained from the extended Born approximation of EFIE and WSHEET due to a vertical magnetic dipole source.

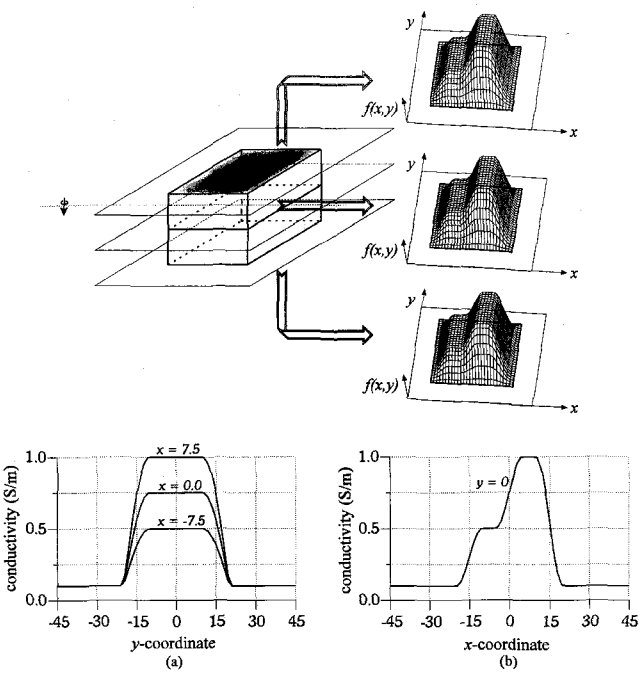

Fig. 12. Composite model which consists of two conductors of conductivity 0.5 and 1.0 S/m, respectively. The conductivity of background medium is 0.1 S/m. Conductivity varies smoothly across the boundary in the form of a sine function. The conductivity profile aong x-axis and y-axis are also shown.

are moving in parallel down the two boreholes.

Figs. 8 and 9 show the real and imaginary components of the secondary magnetic field H_x^s, H_z^s due to HMD source obtained by the extended Born approximation to EFIE. These results are compared with those by WSHEET (Song and Lee, 1998). The lines represent the results from WSHEET and the symbols represent corresponding components from the modeling algorithm of this study. Fig. 8 and 9 show good agreement with WSHEET. Fig. 10 and 11 show the real and imaginary component of the secondary magnetic field, H_x^s, H_z^s due to VMD source obtained by the extended Born approximation and WSHEET. Comparing Fig. 9 with 10, we can notice that the source and receiver reciprocity holds. Fig. 11 shows the real and imaginary components of the secondary vertical magnetic field H_z^s for VMD source. Both real and imaginary components of H_z^s obtained from the extended Born approximation are much higher than those obtained from WSHEET. As shown in Fig. 11, the extended Born approximation solution of the electric field integral equation has serious problems in calcu-

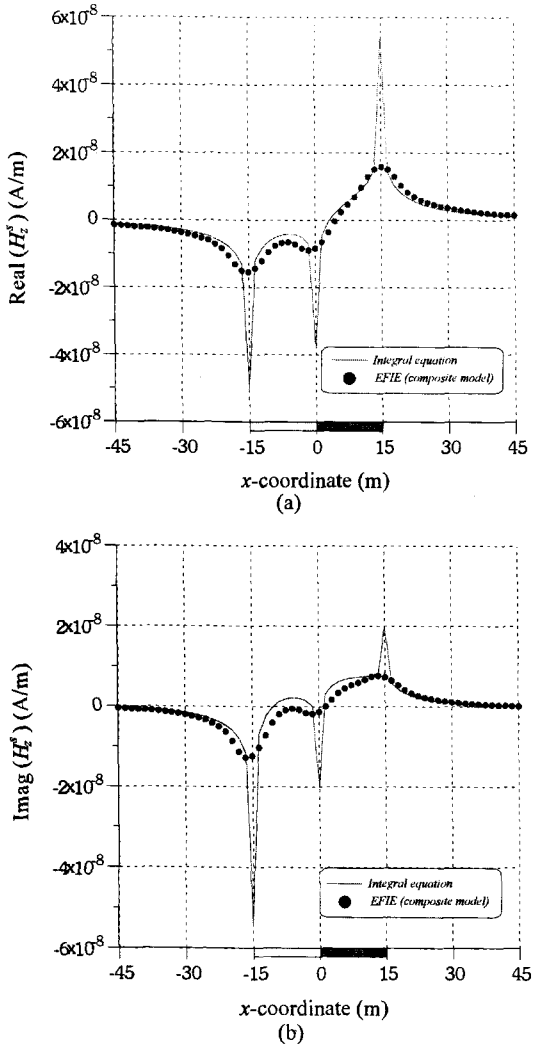

Fig. 13. Comparison of the secondary vertical magnetic field H_z^s obtained from the extended Born approximation of EFIE.
(a) Real component, (b) Imaginary component

lating the response of scattering for above source-receiver configuration.

A composite model

As mentioned earlier, numerical modeling algorithms developed in this study assumes the 3-D conductivity function of a model can be constructed by 2-D functions defined at the planes. This enables us to calculate rather flexible model. Fig. 12 shows a model and its conductivity function. A 30×30×1 m conductor is located at the origin in the whole space of 0.1 S/m. This conductor is composed of two media with different conductivity of 0.5 S/m and 1 S/m. But conductivity function is continuously varying near the interfaces. The various 1-D conductivity profiles with x and y are also shown in (a) and (b). A vertical magnetic dipole is located at (-75,0,0). The electric field of a vertical magnetic field always has tangential component with respect to the surface of a conductor.

The real and imaginary components of vertical magnetic field along x-axis obtained by two modeling algorithms are shown in Fig. 13. The circles denote the results of the extended Born approximation of electric field integral equation. The responses of a composite model obtained from WSHEET are also shown as a dotted line. The responses of the extended Born approximation of the EFIE are close to the results of WSHEET but show smoother curve at the edges of the conductor which results from varying conductivity at the edges. This modeling algorithm developed in this study gives good results for a varying conductivity model.

Conclusions

The main objective of this study is to seek an approximate, but accurate solution rapidly. Most of these approaches are formulated with Born approximation or its variations. The use of these methods can be justified if they can produce reasonably accurate result within measurement error.

In this paper, we developed 3-D EM modeling algorithm using the extended Born approximation of integral equations. Numerical calculations of a Green's tensor integral are performed in (k_x, k_y, z) domain. This approach enables fast computation of Green's tensor integral and gives more flexible description of model construction. Computing time for calculating the responses at 61 by 61 measurement points, for example, a sheet conductor model even takes 75 sec. We showed that this algorithm is accurate over 100 Hz-100 kHz frequency range and 1:16 conductivity contrast. Modeling of composite model which has smoothly varying conductivity has been successful. Care must be done, however, when using extended Born approximation, since the accuracy of extended Born approximation decreases depending on the source and model configurations.

Acknowledgements

We would like to thank Dr. Ki Ha Lee of Berkeley Lab. (Ernest Orlando Lawrence Berkeley National Laboratory) and Yoonho Song of KIGAM (Korea Institute of Geology, Mining and Materials) for helpful suggestions and the permission to use WSHEET code for comparisons. Part of this work was financially supported by the Center of Mineral Resources Research sponsored by KOSEF(Korea Science and Engineering Foundation).

References

1. 조인기, 서정희, 1998, 확장된 Born 근사에 의한 시추공간

전자탐사 2.5차원 모델링: 물리탐사, **1**, 127-135.
2. Alumbaugh, D. L. and Morrison, H. F., 1993, Electromagnetic conductivity imaging with an iterative Born inversion: IEEE Trans. Geosci. Remote Sensing, **31**, 758-763.
3. Alumbaugh, D. L. and Newman, G. A., 1995, Time efficient 3-D electromagnetic modeling on massively parallel computers: Internat. Symp. Three-dimensional electromagnetics: Schlumberger-Doll Research, Expanded Abstracts, 205-218.
4. Coggon, J. H., 1971, Electromagnetic and electrical modeling by the finite element method: Geophysics, **36**, 132-155.
5. Constable S. C., Parker, R. L. and Constable, C. G., 1987, Occam's inversion: A practical algorithm for generating smooth models from electromagnetic sounding data: Geophysics, **52**, 289-300.
6. Habashy, T. M., Groom, R. W. and Spies, B., 1993, Beyond the Born and Rytov approximations: A nonlinear approach to electromagnetic scattering: J. Geophys. Res., **98**, 1759-1775.
7. Hermance, J. F., 1982, Refined finite-difference simulations using local integral forms: Application to telluric fields in two dimensions: Geophysics, **47**, 825-831.
8. Hohmann, G. W., 1975, Three-dimensional induced polarization and electromagnetic modeling: Geophysics, **40**, 309-324.
9. Kong, J. A., 1986, Electromagnetic wave theory: John Wiley & Sons, Inc.
10. Lee, K. H., Pridmore, D. F. and Morrison, H. F., 1981, A hybrid three-dimensional electromagnetic modeling scheme: Geophysics, **46**, 796-805.
11. Lee, S., 1991, Modeling of 3-D electromagnetic responses using time wavenumber method: Ph.D. thesis, Univ. of California, Berkeley.
12. Miller, E. L. and Willsky, A. S., 1996, Wavelet-based methods for the nonlinear inverse scattering problem using the Extended Born Approximation: Radio Sci., **31**, 51-67.
13. Oristaglio, M. L., and Hohmann, G. W., 1984, Diffusion of electromagnetic fields in a two-dimensional earth: A finite-difference approach: Geophysics, **49**, 870-894.
14. Pridmore, D. F., Hohmann, G. W., Ward, S. H. and Sill, W. R., 1981, An investigation of finite-element modeling for electrical and electromagnetic data in three dimensions: Geophysics, **46**, 1009-1024.
15. Song, Y. and Lee, K. H., 1998, A wide-band integral equation solution for EM scattering by thin sheets: 68th Ann. Internat. Mtg., Soc. Expl. Geophys., Expanded Abstracts, 436-439.
16. Tseng, H. W., Lee, K. H. and Becker, A., 1996, An improved numerical technique for 3-D electromagnetic modeling: 66th Ann. Internat. Mtg., Soc. Expl. Geophys., Expanded Abstracts, 249-252.
17. Torres-Verdin, C. and Habashy, T. M., 1994, Rapid 2.5-D forward modeling and inversion via a new non-linear scattering approximation: Radio Sci., **29**, 1051-1079.
18. Torres-Verdin, C. and Habashy, T. M., 1995, A two-step linear inversion of two-dimensional electrical conductivity: IEEE Trans. Ant. Propagation, **43**, 405-415.
19. Walker, P. W. and West, G. F., 1991, A robust integral equation for electromagnetic scattering by a thin plate in conductive media: Geophysics, **56**, 1140-1152.
20. Wannamaker, P. E., Hohmann, G. W. and San Filipo, W. A., 1984, Electromagnetic modeling of three-dimensional bodies in layered earths using integral equations: Geophysics, **49**, 60-74.
21. Ward, S. H. and Hohmann, G. W., 1987, Electromagnetic theory for geophysical applications, in Nabighian, M. N., Ed., Electromagnetic methods in applied geophysics, volume 1, Theory: Soc. Expl. Geophys., Investigations in Geophys., 3.
22. Weidelt, P., 1981, Report on dipole induction by a thin plate in a conductive halfspace with an overburden: Fed. Inst. Earth Sci. and Mate.
23. Xie, G., Lee, K. H. and Li, J., 1995, A new parallel 3-D numerical modeling of the electromagnetic fields: 65th Ann. Internat. Mtg., Soc. Expl. Geophys., Expanded Abstracts, 821-824.
24. Xiong, Z., 1992, Electromagnetic modeling of 3-D structures by the method of system iteration using integral equations: Geophysics, **57**, 1556-1561.
25. Zhou, Q., Becker, A. and Morrison, H. F., 1993, Audio-frequency electromagnetic tomography in 2-D: Geophysics, **58**, 482-495.

Appendix: Whole space tensor Green's function in spatial wavenumber domain

Electric tensor Green's function and magnetic tensor Green's function in spatial wavenumber domain can be derived as the following way. Note that the scalar Green's function satisfies the scalar differential equation

$$\nabla^2 g+k^2 g=-\delta(x-x')\delta(y-y')\delta(z-z'), \tag{A-1}$$

of which solution g is represented as

$$g(r)=\frac{e^{-ikr}}{4\pi r}, \tag{A-2}$$

where $r^2=(x-x')^2+(y-y')^2+(z-z')^2$ (Ward and Hohmann, 1987).

Taking the transform of equation (A-1) and using the derivative property of the Fourier transform results in the equation, one can have

$$(-k_x^2-k_y^2-k_z^2+k^2)\ \tilde{\tilde{\tilde{g}}}=-1. \tag{A-3}$$

Taking inverse Fourier transform of equation (A-3) to evaluate $\tilde{\tilde{\tilde{g}}}\ (k_x, k_y, z-z')$, one can have

$$\tilde{\tilde{\tilde{g}}}(k_x, k_y, z-z')=\frac{1}{2\pi}\int_{-\infty}^{\infty}\frac{1}{k_x^2+k_y^2+k_z^2-k^2}e^{ik_z(z-z')}dk_z. \tag{A-4}$$

Performing integration of equation (A-4) by contour integral, we have

$$\tilde{\tilde{g}}(k_x, k_y, z-z')=\frac{e^{-u|z-z'|}}{2u}, \tag{A-5}$$

where $u^2=k_x^2+k_y^2-k^2$.

Finally we have the electric Green's tensor and magnetic Green's tensor in (k_x, k_y, z) domain by substituting the equation (A-5) into (5), (10)

$$\tilde{\tilde{\underline{G}}}_E(k_x, k_y, z)=\frac{1}{k^2}\begin{bmatrix} k^2-k_x^2 & -k_xk_y & ik_x\frac{\partial}{\partial z} \\ -k_xk_y & k^2-k_y^2 & ik_y\frac{\partial}{\partial z} \\ ik_x\frac{\partial}{\partial z} & ik_y\frac{\partial}{\partial z} & k_x^2+k_y^2 \end{bmatrix}\frac{e^{-u|z-z'|}}{2u} \tag{A-6}$$

and

$$\tilde{\tilde{\underline{G}}}_H(k_x, k_y, z)=\frac{1}{\hat{y}}\begin{bmatrix} 0 & -\frac{\partial}{\partial z} & ik_y \\ \frac{\partial}{\partial z} & 0 & -ik_x \\ -ik_y & ik_x & 0 \end{bmatrix}\frac{e^{-u|z-z'|}}{2u} \tag{A-7}$$

respectively.